

# Post-common envelope PN, fundamental or irrelevant?

Orsola De Marco<sup>1,2</sup>, T. Reichardt<sup>1,2</sup>, R. Iaconi<sup>1,2</sup>, T. Hillwig<sup>3</sup>, G. H. Jacoby<sup>4</sup>, D. Keller<sup>5</sup>, R. G. Izzard<sup>6</sup>, J. Nordhaus<sup>7</sup> and E. G. Blackman<sup>8</sup>

<sup>1</sup>Department of Physics & Astronomy, Macquarie University, Sydney, NSW 2109, Australia  
email: orsola.demarco@mq.edu.au

<sup>2</sup>Astronomy, Astrophysics and Astrophotonics Research Centre, Macquarie University

<sup>3</sup>Department of Physics & Astronomy, Valparaiso University, Indiana, USA

<sup>4</sup>Lowell Observatory, Flagstaff, AZ, USA

<sup>5</sup>KU Leuven, Belgium

<sup>6</sup>Institute of Astronomy, Cambridge University, UK

<sup>7</sup>National Technical Institute for the Deaf, Rochester Institute of Technology, NY, USA

<sup>8</sup>University of Rochester, NY, USA

**Abstract.** One in 5 PN are ejected from common envelope binary interactions but *Kepler* results are already showing this proportion to be larger. Their properties, such as abundances can be starkly different from those of the general population, so they should be considered separately when using PN as chemical or population probes. Unfortunately post-common envelope PN cannot be discerned using only their morphologies, but this will change once we couple our new common envelope simulations with PN formation models.

**Keywords.** planetary nebulae: general, hydrodynamics, stars: AGB and post-AGB, binaries (including multiple): close, stars: evolution, stars: statistics

---

## 1. The fraction and chemistry of post-common envelope PN

At least one in 5 planetary nebulae (PN) derives from a common envelope (CE) binary interaction, where the PN is the ejected CE and the inner close binary is the result of the companion's in-spiral into the progenitor AGB stars (Ivanova et al. 2013). This fraction is a lower limit because we cannot detect photometric variabilities  $\lesssim 0.1$  mag, due primarily to poor sampling of ground-based observations. A search carried out with the *Kepler Space Telescope* resulted in the detection of 4 variables out of 5 objects with data (De Marco et al. 2015). Of the 4 variables, one is a double-degenerate binary central star, and one is likely to be a pole-on binary. With variability amplitudes of 0.0007 and 0.0005 mag, neither would have been detected from the ground.

A binary search using data from *Kepler II* (K2), campaigns 0, 2, 7 and 11 is underway. Campaigns 0, 2 and 7 include a grand total of 15 PN, two of which have periodic variability consistent with binarity. The variability amplitudes, 0.05 and 0.02 mag, respectively, are at the low end of what could be detected from the ground. However, the sensitivity of K2 is up to 5 times worse than for *Kepler* and neither of the 2 binaries detected with *Kepler* would have been detected by K2. In addition, 11 of the 15 K2 targets analysed are compact PN, while all the *Kepler* targets are extended: the variability detection threshold is therefore much worse for the bulk of the K2 targets. K2, Campaign 11 has 139 PN on silicon of which 22 are extended. Hopefully those data will return better statistics. The *Kepler* data show that low amplitude post-CE PN central binaries exist, as predicted and that the fraction of post-CE PN could be substantially larger than the lower limit of

one in 5. This lower limit is already larger than the prediction from population synthesis of 9% for Solar metallicity of Izzard & Keller (2015, which are consistent with previous work, e.g., Yungelson et al. (1993); Nie et al. (2012)). An over-abundance of post-CE PN could be explained either if some single stars make under-luminous PN (Soker & Subag 2005) or if some post-CE PN are mimics, such as for example Stroemgren spheres around hot stars (Frew & Parker 2010).

Expectations of the properties of post-CE PN are different from those of PN from other evolutionary channels. Post-CE PN have a curbed AGB evolution, resulting in reduced C/O ratios and lower s-process abundances. A secondary effect is that more massive stars are in binaries more often, something that could inflate the relative number of more massive stars in the post-CE PN population resulting in relatively larger N/O ratios. In Fig. 2 we can compare the top-left and bottom-right panels where we see the relatively broader distributions in the post-CE channel and also the larger, though still small, proportion of PN at high N/O and very low C/O not present in the single star channel. The observations are still insufficient for a proper comparison, but it is already clear that the observed bipolar PN at low C/O and mostly but not exclusively high N/O (more massive central stars) can only be (approximately) reproduced by the CE channel.

## 2. Observed and simulated post-common envelope PN

Unfortunately we cannot unambiguously recognise post-CE PN based on their morphology alone. Approximately 50 post-CE central stars are known to date and about two thirds of them are reasonably well imaged. As shown by Miszalski et al. (2009), many of these PN are approximately bipolar (e.g., A 41, A 79, K 1-2, Fig.2), but there is some diversity. Some PN display only a narrow waist (e.g., HaTr 4), sometimes with jets (A 63; jets not visible in Fig. 2). Ring nebulae (e.g., NGC 6337, Sp 1) are likely to be pole-on views of waists. More complex morphologies are also present: elliptical PN with jets (NGC 6778, Fleming 1), more or less elliptical distributions of faint gas on which we

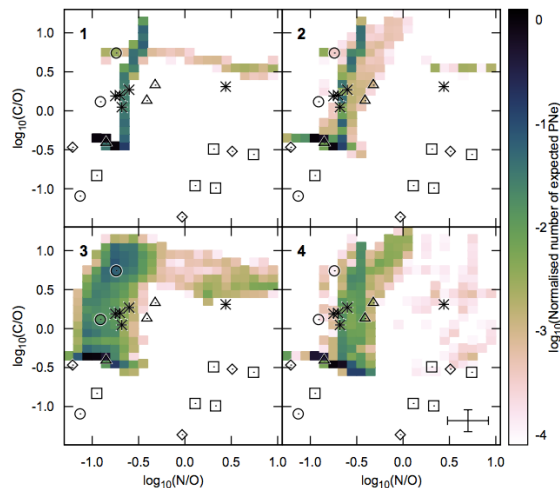


**Figure 1.** Observed vs. predicted C/O and N/O ratios for PN produced via different channels: (1) single stars, (2) wind mass-loss from binary star origin, (3) CE merger + wind mass loss, (4) CE ejection. Observation symbols: round: round PN; star: elliptical PN; square: bipolar PN; triangular: elliptical PN with bipolar core, rhomboid: quadrupolar PN. Observations: Leisy & Dennefeld (2006); Stanghellini et al. (2005). Figure from Keller, Izzard and Stanghellini, in prep.

see superimposed stark and very collimated double (K 1-2, PN G 135.9) or single jet-like structures (HFG 1, M 2-29).

The only way to understand how these shapes result from CE ejections is via simulations, such as those by García-Segura et al. (1999) or Huarte-Espinosa et al. (2012). Nobody to date has simulated a post-CE PN *accounting for the common envelope ejection*. Simulations of the CE interaction have shown that the ejection of the envelope takes place primarily on the orbital plane (Sandquist et al. 1998; Passy et al. 2012). We have recently carried out a 2-million particle SPH simulation with the code PHANTOM (Iaconi et al. 2017) and the parameters of Passy et al. (2012), but starting the simulation at the time of Roche lobe overflow, something that allows the distribution of ejected gas to be more realistic. In addition, with SPH the entire gas distribution at the end of the simulation ( $\sim 15$  years after Roche lobe overflow) is known, albeit with varying resolution (from  $0.3 R_{\odot}$  near the binary to  $80 R_{\odot}$  near the outer parts of the distribution).

This simulation has not considered the fast wind, nor the ionising radiation. We could plausibly assume that the central star at the end of our simulation is hotter than  $\sim 20,000$  K. If so, both ionising radiation and a fast tenuous wind would start blowing into the dense CE structure. While this has not been done yet in these simulations, using this image we can already make the following considerations. If a fast wind were to start at the end of the CE in-spiral it would meet with incredibly high densities, of the order of  $10^{-8} \text{ g cm}^{-3}$  in the vicinity of the stars (Fig. 3, left panel). Even the evacuated, funnel-like regions seen above and below the equatorial plane have high densities ( $\sim 10^{-11} \text{ g cm}^{-3}$ ). By comparison typical PN simulations blow a fast wind into a much more tenuous medium with typical densities of  $10^{-21} \text{ g cm}^{-3}$ , e.g., García-Segura (2006). This shows that the CE structure presents more or less a solid wall to the fast wind. On

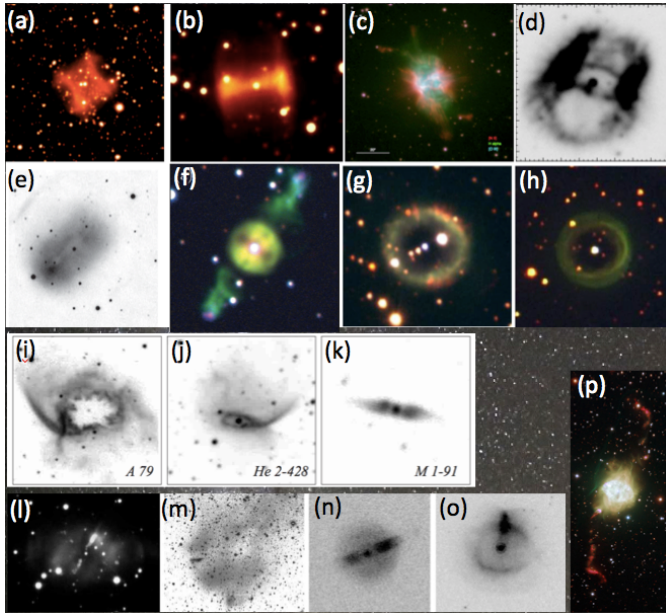


**Figure 2.** PN around post-CE central binaries; (a) A 63 (Mitchell et al. 2007); (b) HaTr 4 (from the ESO NTT archive); (c) NGC 6778 (Guerrero & Miranda 2012); (d) A 41 (Jones et al. 2010); (e) A 65 (Huckvale et al. 2013); (f) ETHOS 1 (Miszalski et al. 2011); (g) NGC 6337 (Hillwig et al. 2010); (h) Sp 1 (Hillwig et al. 2016); (i) A 79, (j) He 2-428, (k) M 1-91 (Rodríguez et al. 2001); (l) K 1-2 (Corradi et al. 1999); (m) HFG 1 (De Marco 2009); (n) PN G135.9+55.9 (Napiwotzki et al. 2005); (o) M 2-29 (Hajduk et al. 2008); (p) Fleming 1 (Boffin et al. 2012).

the other hand the entire CE is expanding at a range of speeds with the bulk of the volume expanding at  $20 \text{ km s}^{-1}$ . Hence, in 100-1000 years the densities will decline by 5 to 8 orders of magnitude and the wind will start sweeping and penetrating the CE.

## References

- Boffin, H. M. J., Miszalski, B., Rauch, T., Jones, D., et al. 2012, *Science*, 338, 773  
 Corradi, R. L. M., Perinotto, M., Villaver, E., Mampaso, A., et al. 1999, *ApJ*, 523, 721  
 De Marco, O. 2009, *PASP*, 121, 316  
 De Marco, O., Long, J., Jacoby, G. H., Hillwig, T., et al. 2015, *MNRAS*, 448, 3587  
 Frew, D. J. & Parker, Q. A. 2010, *PASA*, 27, 129  
 García-Segura, G. 2006, in *IAU Symposium*, Vol. 234, ed. M. J. Barlow & R. H. Méndez, 297–304  
 García-Segura, G., Langer, N., Różyczka, M., & Franco, J. 1999, *ApJ*, 517, 767  
 Guerrero, M. A. & Miranda, L. F. 2012, *A&A*, 539, A47  
 Hajduk, M., Zijlstra, A. A., & Gesicki, K. 2008, *A&A*, 490, L7  
 Hillwig, T. C., Bond, H. E., Afşar, M., & De Marco, O. 2010, *AJ*, 140, 319  
 Hillwig, T. C., Jones, D., De Marco, O., Bond, H. E., et al. 2016, *ApJ*, 832, 125  
 Huarte-Espinosa, M., Frank, A., Balick, B., Blackman, E. G., et al. 2012, *MNRAS*, 424, 2055  
 Huckvale, L., Prouse, B., Jones, D., Lloyd, M., Pollacco, D., et al. 2013, *MNRAS*, 434, 1505  
 Iaconi, R., Reichardt, T., Staff, J., De Marco, O., Passy, J.-C., et al. 2017, *MNRAS*, 464, 4028  
 Ivanova, N., Justham, S., Chen, X., De Marco, O., et al. 2013, *A&A Rev.*, 21, 59  
 Izzard, R. G. & Keller, D. 2015, in *ASPCS*, Vol. 497, ed. Kerschbaum, Wing, Hron, 161  
 Jones, D., Lloyd, M., Santander-García, M., López, J. A., et al. 2010, *MNRAS*, 408, 2312  
 Leisy, P. & Dennefeld, M. 2006, *A&A*, 456, 451  
 Miszalski, B., Acker, A., Parker, Q. A., Boffin, H. M. J., Frew, D. J., et al. 2011, in *APN5*, 109  
 Miszalski, B., Acker, A., Parker, Q. A., & Moffat, A. F. J. 2009, *A&A*, 505, 249  
 Mitchell, D. L., Pollacco, D., O’Brien, T. J., Bryce, M., et al. 2007, *MNRAS*, 374, 1404  
 Napiwotzki, R., et al. 2005, in *AIPCS*, Vol. 804, ed. Szczerba, Stasinska, & Gorny, p. 173  
 Nie, J. D., Wood, P. R., & Nicholls, C. P. 2012, *MNRAS*, 423, 2764  
 Passy, J.-C., De Marco, O., Fryer, C. L., Herwig, F., Diehl, S., et al. 2012, *ApJ*, 744, 52  
 Rodríguez, M., Corradi, R. L. M., & Mampaso, A. 2001, *A&A*, 377, 1042  
 Sandquist, E. L., Taam, R. E., Chen, X., Bodenheimer, P., & Burkert, A. 1998, *ApJ*, 500, 909  
 Soker, N. & Subag, E. 2005, *AJ*, 130, 2717  
 Stanghellini, L., Shaw, R. A., & Gilmore, D. 2005, *ApJ*, 622, 294  
 Yungelson, L. R., Tutukov, A. V., & Livio, M. 1993, *ApJ*, 418, 794

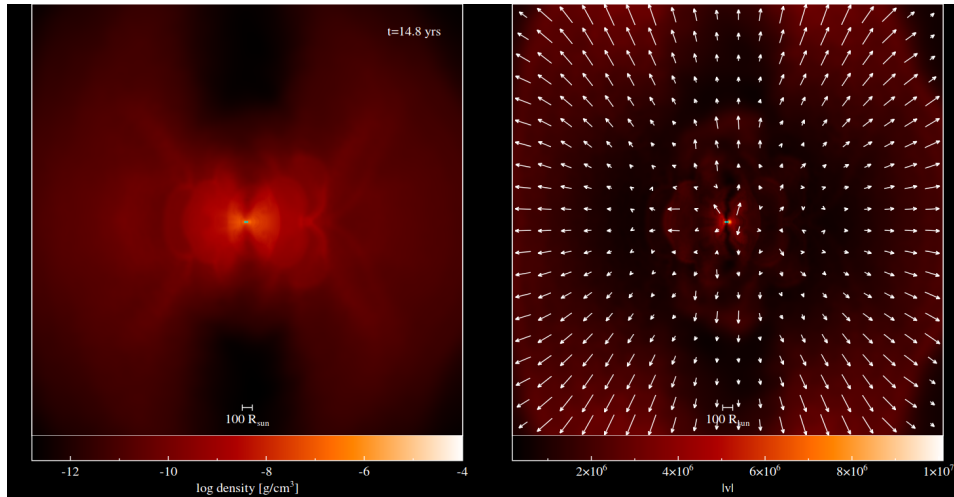


**Figure 3.** Density (left) and velocity (right, in  $\text{cm s}^{-1}$ ; arrows indicate flow direction) slices perpendicular to the orbital plane at 14.8 years of an SPH CE simulation between a  $0.88 M_{\odot}$ , RGB star and a  $0.6 M_{\odot}$  companion, carried out with the PHANTOM code (Iaconi et al. 2017).